

# Crystal Structure of B-Amylose

Yasuhiro Takahashi,\* Takeshi Kumano, and Sumiyo Nishikawa

Department of Macromolecular Science, Graduate School of Science, Osaka University, Toyonaka, Osaka 560-0043, Japan

Received May 8, 2004; Revised Manuscript Received June 22, 2004

**ABSTRACT:** A fiber specimen of B-amylose was prepared from enzymatically synthesized amylose, which is a purely linear 1,4-linked poly- $\alpha$ -D-glucose. X-ray crystal structure analysis was carried out by using the newly collected intensity data, which was estimated by using imaging plate according to the new procedure. The molecule of B-amylose assumes a left-handed parallel strand double helix, and two double helices pass through a hexagonal unit cell with parameters  $a = b = 18.52 \text{ \AA}$ ,  $c$  (fiber axis) =  $10.57 \text{ \AA}$ ,  $\gamma = 120^\circ$ , and the space group  $P6_1-C_6^2$ . A total of 36 water molecules were contained in a unit cell. The conformation of the primary hydroxyl group is gg, and the conformation of the bonds linking two glucose residues,  $\Phi$  and  $\Psi$ , are  $+84.3$  and  $-135.2^\circ$ , respectively.

## Introduction

Amylose is  $\alpha$ -1,4-D-glucan: a linear polymer of  $\alpha$ -1,4-D-glucose and a main component of starch.<sup>1–5</sup> The polymorphs in amylose are classified as A, B, C, and V in the same way as starch. Form A is found in corns and form B is found in potatoes. Form C is found in peas and banana and is known to be the mixed crystal of A and B. Many structural studies have been done on amylose so far. Wu and Sarko reported that, in forms A<sup>1,2</sup> and B,<sup>5</sup> the molecule assumes the right-handed double strand helix and packs in antiparallel manner, while Imberty et al. reported that, in forms A<sup>6,7</sup> and B,<sup>8</sup> the molecule assumes the left-handed double strand helix and packs in parallel manner. On the other hand, in form V, the molecule assumes left-handed single (6/1)helix.<sup>9–10</sup> The structures of oligomers of amylose<sup>12–14</sup> methyl- $\alpha$ -maltotriose of three glucose residues and cyclomaltotetraose of four glucose residues support the structure of form V.

In the previous paper,<sup>15</sup> the crystal structure of amylose triacetate I was clarified by using the enzymatically synthesized amylose. In this crystal, two left-handed (14/3) helices deviated from helical symmetry pass through the orthorhombic unit cell with parameters,  $a = 10.92 \text{ \AA}$ ,  $b = 18.91 \text{ \AA}$ ,  $c$  (fiber axis) =  $53.91 \text{ \AA}$ , and the space group  $P2_12_12_1$ . Up- and down-pointing molecules statistically occupied a crystal site with the ratio 0.87:0.13.

In the present study, the crystal structure of B amylose was analyzed by X-ray diffraction method. It was clarified that two left-handed double strand helices pass through a hexagonal unit cell with parameters,  $a = b = 18.52 \text{ \AA}$ ,  $c$  (fiber axis) =  $10.57 \text{ \AA}$ , and the space group  $P6_1$ , in parallel manner.

## Experimental Section

**Sample.** Usually, natural amylose obtained from starch contains a small amount of impurity: amylopectin in addition to a small amount of branch attached by (1–6)- $\alpha$  linkage. On the other hand, enzymatically synthesized amylose is purely linear (1–4)- $\alpha$ -D-glucan.<sup>16,17</sup> In the present study, enzymatically synthesized amylose was kindly supplied by Prof. S. Kitamura of Osaka Prefectural University. The procedures for the preparation of B form are essentially the same as in the reported one.<sup>5,18–21</sup> First, amylose triacetate was prepared by the method described in the previous paper,<sup>15</sup> and the oriented

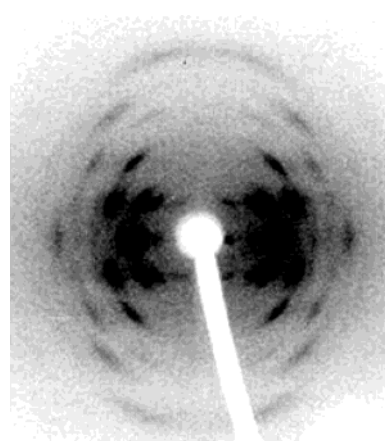


**Figure 1.** Fiber diagram of B-amylose taken by imaging plate.

film of amylose triacetate was prepared by stretching in glycerine bath at  $170^\circ\text{C}$ . The oriented film thus obtained was deacetylated by soaking it in a mixture of 0.2 M potassium hydroxide and 75% ethanol at room temperature for 24 h. under tension. Furthermore, the alkaline solution on the sample was wiped, and the ethanol was evacuated by aspirator under 100% relative humidity. The sample was kept under 80% relative humidity (saturated ammonium chloride solution) at room temperature for 3 days and furthermore, was kept under 100% relative humidity at room temperature for 3 days. Finally, the sample was kept in autoclave along with water at  $100^\circ\text{C}$  for 1 h. X-ray diffraction pattern of this sample corresponds to that of B amylose.

**X-ray Measurements.** X-ray measurements were carried out by Cu  $K\alpha$  radiation monochromatized by a pyrolyzed graphite. Fiber diagrams were taken by imaging plate with a cylindrical camera with 5.0 cm radius in the stream of He gas passed through potassium sulfate saturated aqueous solution (98% r. h.). Weissenberg diagrams were taken by imaging plate with cylindrical camera with 4.5 cm radius according to Norman's method.<sup>22</sup> The fiber and Weissenberg diagrams are shown in Figures 1 and 2, respectively.

Integrated intensities were estimated by the following procedures,<sup>23,15,24,25</sup> in the same way as by the drum scan densitometer procedures of X-ray films.<sup>26–28</sup> First, the digital data for one pixel ( $100 \mu\text{m}^2$ ) of the reflection are summed up along the arc with constant  $2\theta$ , and the summed intensities are plotted against a layer line. Then, from the one-dimensional intensity curve thus obtained, the integrated intensity was estimated. For overlapped reflections, one-dimensional intensity curve was fitted and separated under the assumption

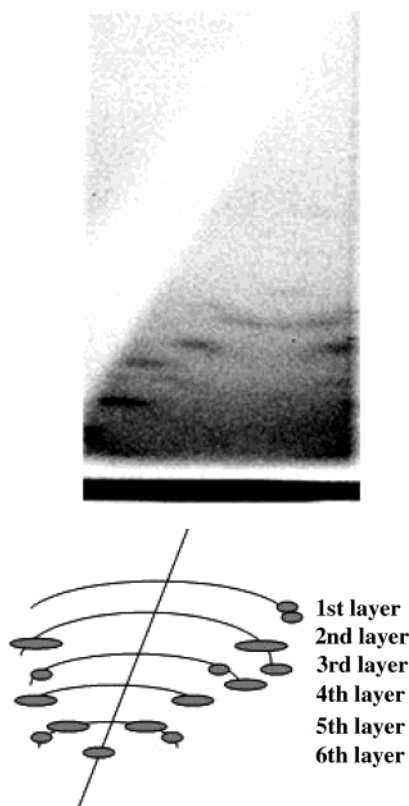


**Figure 2.** Weissenberg diagram of B-amylose taken by imaging plate.

of pseudo-Voigt function: a linear combination of Gauss and Cauchy functions.<sup>29</sup> Thus, the integrated intensities of 38 reflections could be estimated.

**Density.** Density measurement was made by the flotation method at 25 °C. Small particles of B-amylose sample were inserted into a mixture of 1,4-dioxane and chloroform, and 1,4-dioxane and chloroform were added alternatively until the particles stopped in the mixture. Then, the density of the mixture was measured by using a DMA500 (Anton Paar). The density of B-amylose was thus estimated as 1.362 g/cm<sup>3</sup>.

## Results and Discussion

**Unit Cell and Space Group.** All the observed reflections can be indexed by the hexagonal unit cell with  $a = b = 18.52$  Å,  $c$  (fiber period) = 10.57 Å, and  $\gamma = 120^\circ$ . On the meridian of the Weissenberg diagram (Figure 2), only the 006 reflection is observed. This suggests that the systematic absence  $l \neq 6n$  exists for 00 $l$  reflections. No other systematic absences were found. Therefore, this suggests that the space group is the one of the following four possible space groups:  $P6_1$ ,  $P6_5$ ,  $P6_122$ , and  $P6_522$ . The number of general equivalent positions is 6 for  $P6_1$  and  $P6_5$  and is 12 for  $P6_122$  and  $P6_522$ . Accordingly, the number of glucose residues contained in a unit cell may be 6, 12, or 18, for which the calculated densities are 0.5147, 1.0294, and 1.5441 g/cm<sup>3</sup>, respectively. From the observed density 1.362 g/cm<sup>3</sup>, the unit cell is concluded to contain 12 glucose residues. Furthermore, when 30, 36, and 42 water molecules are contained in the unit cell, the densities are calculated as 1.3153, 1.3726, and 1.4298 g/cm<sup>3</sup>, respectively. This suggests that the unit cell contains 36 water molecules.

**Crystal Structure Models.** In Figure 3, the symmetries and the molecular packing in the space group  $P6_1$  are shown. Two double strand helices locate on two

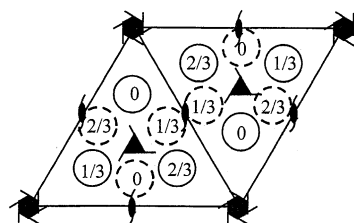


**Figure 3.** Symmetries and the molecular packing in the space group  $P6_1$ .

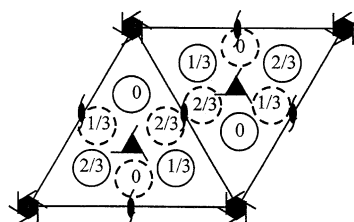


**Figure 4.** Symmetries and the molecular packing in the space group  $P6_5$ .

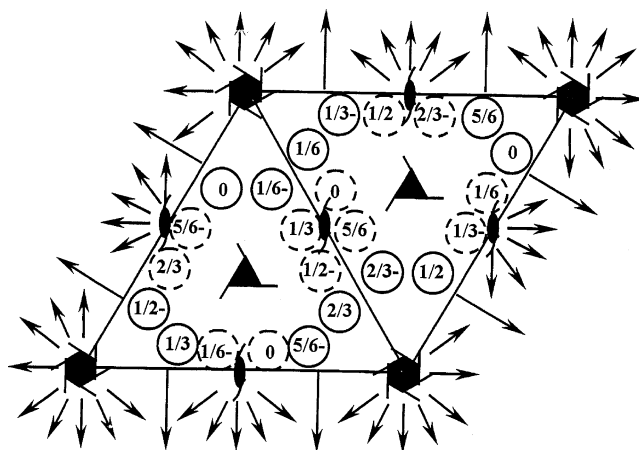


**Figure 5.** Symmetries and the molecular packing in the space group  $P6_122$ .

$3_1$  helices of the space group, where the solid circles with heights, 0,  $1/3$ , and  $2/3$  show the general equivalent positions of the space group  $P6_1$ . The dashed circle with heights, 0,  $1/3$ , and  $2/3$  are generated by the postulated 2-fold rotation axis coinciding with the  $3_1$  screw axis according to Imberty and Perez.<sup>8</sup> One glucose residue is allotted to each circle. Accordingly, one asymmetric unit consists of two glucose residues. One single helix in the double strand helix is given by the solid circle with height 0, the dashed circle with height  $1/3$ , and the solid circle with height  $2/3$ , and the other single helix in the double strand helix is given by the dashed circle with height 0, the solid circle with height  $1/3$ , and the dashed circle with height  $2/3$ . Accordingly, in the case of the space group  $P6_1$ , the single helix is left-handed ( $6_1$ ) helix with symmetry  $6_5$  and fiber period  $2c = 21.14$  Å. Two single helices in a double helix are stranded in parallel manner. Two double strand helices in the unit cell pack in parallel manner because two  $3_1$  helices in the unit cell possess the same circumference. That is to say, in the case of the space group  $P6_1$ , two left-handed parallel-stranded double helices pass through a unit cell in parallel manner. In the case of the space group  $P6_5$ , two right-handed parallel-stranded double helices pass through a unit cell in parallel manner (Figure 4). The symmetries and the molecular packing in the space groups  $P6_122$  and  $P6_522$  are shown in Figures 5 and 6,

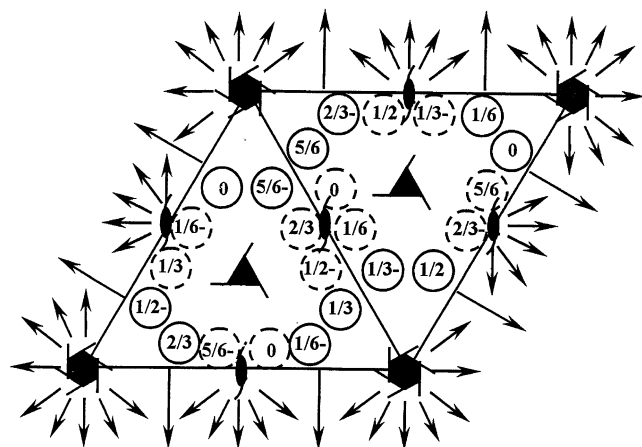


**Figure 6.** Symmetries and the molecular packing in the space group  $P6_522$ .

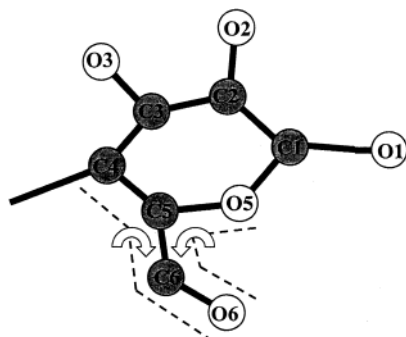


**Figure 7.** Conformation of the primary hydroxyl group.

respectively. In these space groups, there exist 2-fold rotation axes perpendicular to the  $6_1$  and  $6_5$  helix axes, and therefore, the up-pointing and down-pointing double strand helices are statistically located on the  $3_1$  helix axes of the space groups with 1:1 ratio. In Figure 5, the solid circles show the general equivalent positions of the space group  $P6_122$ , and the dashed circles are generated by the postulated 2-fold rotation axis coinciding with  $3_1$  helix axis. The up-pointing double strand helix is composed of two single helices: one is given by the solid circle with height 0, the dashed circle with height  $1/3$ , and the solid circle with height  $2/3$  and the other is given by the dashed circle with height 0, the solid circle with height  $1/3$ , and the dashed circle with height  $2/3$ . The down-pointing double strand helix is also composed of two single helices: one is given by the solid circle with height  $1/6$ , the dashed circle with height  $1/2$ , and the solid circle with height  $5/6$ , and the other is given by the dashed circle with height  $1/6$ , the solid circle with height  $1/2$ , and the dashed circle with height  $5/6$ . Accordingly, in the case of  $P6_122$ , the up- and down-pointing molecules of left-handed parallel-stranded double helix statistically occupy the  $3_1$  helix axes of the space group with 1:1 ratio. In the case of  $P6_522$ , the up- and down-pointing molecules of right-handed parallel-stranded double helix statistically occupy the  $3_1$  helix axes of the space group with 1:1 ratio (Figure 6). On the other hand, there are three possible conformations for the primary hydroxyl group around the C(5)–C(6) bond: gauche–trans (gt), gauche–gauche (gg), and trans–gauche (tg), which are the internal rotation angle O(5)–C(5)–C(6)–O(6) followed by the internal rotation angle C(4)–C(5)–C(6)–O(6) (Figure 7). Consequently, 12 crystal structure models were built up.

**Table 1.** Bond Lengths, Bond Angles, and Internal Rotation Angles for Ring Atoms of B-Amylose

Ring Bond Lengths (Å)			
C4–O4	1.426	O1–C1	1.415
C4–C3	1.523	O5–C1	1.414
O3–C3	1.429	C5–O5	1.436
C2–C3	1.521	C6–C5	1.514
O2–C2	1.423	O6–C6	1.427
C1–C2	1.523	C4–C5	1.525
Ring Bond Angles (deg)			
O4–C4–C3	110.4	C2–C1–O5	109.2
C4–C3–O3	109.7	C5–O5–C1	114.0
C4–C3–C2	110.5	C6–C5–O5	106.9
C3–C2–O2	110.8	O6–C6–C5	111.8
C3–C2–C1	110.5	C4–C5–O5	110.0
C2–C1–O1	108.4	C5–C4–C3	110.3
Ring Internal Rotation Angles (deg)			
C4–C3–C2–C1	–53.2	C1–O5–C5–C4	61.1
C3–C2–C1–O5	56.0	O5–C5–C4–C3	–55.4
C2–C1–O5–C5	–62.2	C5–C4–C3–C2	53.0

**Table 2.** Distances (Å) Constrained by Lagrange's Undetermined Multipliers between Two Neighboring Residues

C1...O1'	1.415
C1...C4'	2.327
C2...O1'	2.415

**Refinements of Amylose Molecules.** There may exist two approaches to the crystal structure analysis of biopolymers including polysaccharide containing water molecules. The first approach is that the biopolymer molecule is surrounded by a large amount of water and the positions of water molecules are completely disordered, and therefore, the water-weighted atomic scattering factors are adopted. The second is that the water molecules occupy the definite positions in the unit cell and therefore, the positions of water molecules are refined independently of the biopolymer molecules themselves. The density measurement in the present study suggests that water is contained only three molecules per one glucose residue which is composed of 6 carbon atoms, 5 oxygen atoms, and 10 hydrogen atoms. Therefore, the water molecules are considered to occupy the definite positions in unit cell. This was supported by the previous works reported by Wu and Sarko<sup>5</sup> and Imberty and Perez.<sup>8</sup> In the present study, the second approach was adopted, and first, the amylose molecule was refined and the water molecules were refined independently of the amylose molecules.

The structure refinements of the amylose molecules were carried out by using the constrained least-squares method<sup>28,30</sup> for the observed reflection intensities. Here, the bond lengths, bond angles, and internal rotation angles for ring atoms were fixed on the values listed in Table 1, which are determined in the reference of the work reported by Arnott and Scott.<sup>31</sup> The bond lengths and bond angles between two glucose residues are fixed on the values given in Table 2 by using Lagrange's undetermined multipliers. Furthermore, the 2-fold rotation axes were located on the  $3_1$  helix axes of the space group as the pseudo-symmetry. Accordingly, the parameters to be refined are the coordinates of the origin atom,  $x$  and  $y$ , three Eulerian angles,  $\theta$ ,  $\varphi$ , and  $\chi$ , which relates the coordinates fixed on the molecule to those fixed on the unit cell, the internal rotation angle of the primary hydroxyl group  $\tau$ , the overall temperature factor  $B$ , and the scale factor  $S$ . In the cases of the space groups  $P6_122$  and  $P6_522$ , the coordinate of the origin atom  $z$  was added to the above-mentioned parameters.



**Table 3. Discrepancy Factors (%) for the Converged Models for B-Amylose**

Left-Handed Helix		
$P6_1$ -gg		30.45
$P6_1$ -tg		30.93
$P6_1$ -gt		36.01
Right-Handed Helix		
$P6_5$ -gg		34.97
$P6_5$ -tg		34.92
$P6_5$ -gt		36.36
Left-Handed Helix		
$P6_{122}$ -gg		40.36
$P6_{122}$ -tg		39.25
$P6_{122}$ -gt		42.78
Right-Handed Helix		
$P6_{522}$ -gg		40.81
$P6_{522}$ -tg		37.91
$P6_{522}$ -gt		38.77

**Table 4. Discrepancy Factors (%) for the Converged Models  $P6_1$  and  $P6_5$  Including Water Molecules**

Left-Handed Helix		
$P6_1$ -gg		10.85
$P6_1$ -tg		14.79
$P6_1$ -gt		16.86
Right-Handed Helix		
$P6_5$ -gg		15.08
$P6_5$ -tg		13.10
$P6_5$ -gt		21.18

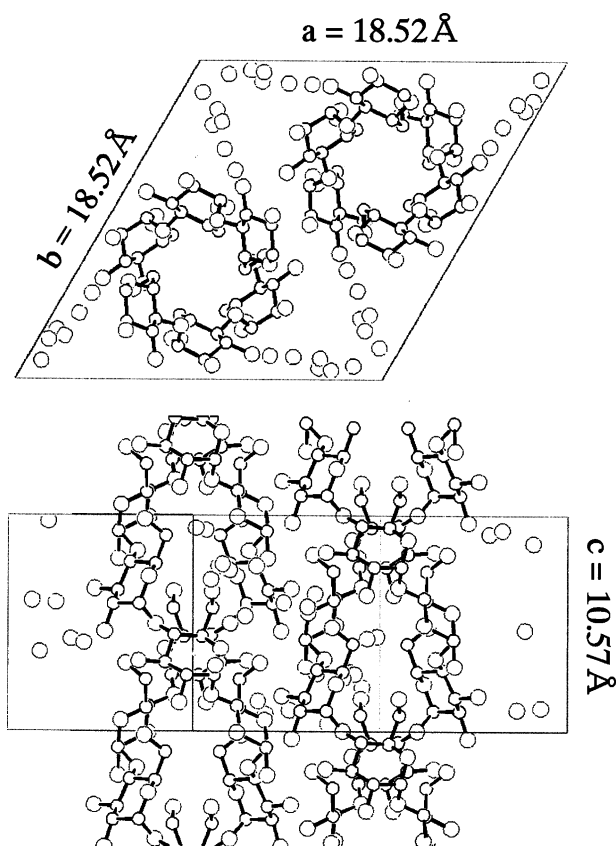
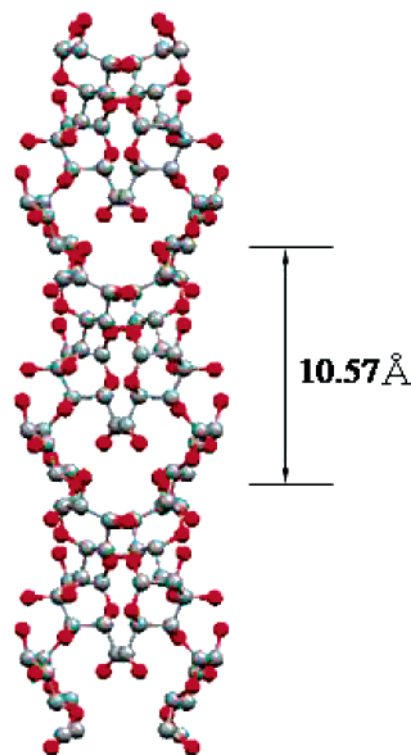
**Table 5. Discrepancy Factors (%) for the Converged Models  $P6_{122}$  and  $P6_{522}$  Including water molecules**

Left-Handed Helix		
3H <sub>2</sub> O		
$P6_{122}$ -gg		21.39
$P6_{122}$ -tg		28.30
$P6_{122}$ -gt		21.97
6H <sub>2</sub> O		
$P6_{122}$ -gg		20.96
$P6_{122}$ -tg		28.30
$P6_{122}$ -gt		21.97
Right-Handed Helix		
3H <sub>2</sub> O		
$P6_{522}$ -gg		24.57
$P6_{522}$ -tg		28.47
$P6_{522}$ -gt		26.16
6H <sub>2</sub> O		
$P6_{522}$ -gg		24.26
$P6_{522}$ -tg		27.29
$P6_{522}$ -gt		24.40

**Table 6. Parameters by the Constrained Least Squares Refinement for  $P6_1$ -gg Model of B-Amylose without Water Molecules**

	value	standard deviation
Fractional Coordinates of the Origin Atom C1		
<i>x</i>	0.499	0.005
<i>y</i>	0.798	0.008
<i>z</i>	0.000	fix
Eulerian Angles (deg)		
$\theta$	99.0	2.1
$\varphi$	10.7	3.6
$\chi$	-292.6	1.9
Internal Rotation Angle of Hydroxyl Group (deg)		
$\tau$	-65.1	14.9
Overall Temperature Parameter		
<i>B</i>	-8.54	10.89

The results are given in Table 3. The crystal structure model of  $P6_1$  with gauche-gauche conformation gives the lowest *R* factor 30.4%. However, all the *R* factors are not sufficiently low to judge which model is correct.

**Figure 8.** Crystal structure of B-amylose.**Figure 9.** Molecular structure of B-amylose.

**Refinements of Water Molecules.** The refinements of the water molecules are carried out by using the usual full matrix least-squares method.<sup>32</sup> Here, the fractional coordinates of the amylose molecules are fixed and only the fractional coordinates of the oxygen atoms of water molecules are refined. A unit cell contains 36 water

**Table 7. Comparison between the Observed and Calculated Structure Factors**

index	$\sqrt{I_o}$	$\sqrt{I_c}$	index	$\sqrt{I_o}$	$\sqrt{I_c}$	index	$\sqrt{I_o}$	$\sqrt{I_c}$
100	140.2	295.7	071	-	251.1	053	365.8	336.7
110	-	96.7	261	-	420.6	243	-	-
200	187.1	149.8	621	-	4.8	423	-	-
120	348.5	342.3	171	-	98.2	333	-	-
210	-	-	711	-	149.1	153	-	130.4
300	524.4	502.8	361	-	89.0	513	-	154.4
130	488.2	514.2	631	-	45.7	253	-	92.9
310	-	-	451	-	236.4	523	-	74.4
220	-	-	541	-	84.3	343	-	55.2
040	-	78.7	271	-	226.1	433	-	129.9
230	-	186.4	721	-	296.8	063	-	39.2
320	-	89.9	081	-	290.7	163	-	261.8
140	169.5	157.9	181	432.4	422.9	613	-	184.3
410	-	-	811	-	-	353	343.1	347.4
050	-	193.5	461	-	-	533	-	-
240	387.7	364.3	641	-	-	443	-	-
420	-	-	551	-	-	073	-	-
330	-	-	012	-	93.4	014	-	80.5
150	-	375.6	022	425.3	223.2	114	-	236.4
510	-	296.3	112	-	-	024	-	92.4
600	493.5	488.9	032	569.0	451.6	124	674.9	719.6
250	-	-	122	-	-	214	-	-
520	-	-	212	-	-	034	-	-
340	-	-	222	-	97.6	224	-	-
430	-	-	132	150.6	146.5	044	-	123.7
101	137.8	121.8	312	-	-	234	-	219.0
021	353.5	341.6	042	300.3	257.1	324	-	243.2
111	-	-	232	-	-	134	177.2	176.1
121	528.0	453.4	322	-	-	314	-	-
211	-	-	142	420.6	415.5	054	-	97.0
031	-	-	412	-	-	334	-	259.0
131	461.1	443.9	052	-	170.5	144	173.1	168.4
311	-	-	332	-	84.4	414	-	-
221	-	-	242	269.3	297.9	244	306.4	312.1
041	398.7	383.7	152	-	-	424	-	-
231	209.2	278.1	512	-	-	154	-	84.3
321	-	-	062	-	269.2	514	-	236.2
141	-	-	342	-	237.3	344	-	90.6
411	-	-	432	-	199.2	434	-	110.7
051	-	135.5	252	190.2	228.1	064	-	351.1
331	-	36.9	522	-	-	254	144.1	197.1
241	369.0	368.9	013	-	29.8	524	-	-
421	-	-	113	-	116.5	015	-	355.6
151	-	235.0	023	-	163.2	115	-	240.5
511	-	80.2	123	380.7	254.4	025	-	325.1
061	262.5	302.7	213	-	-	035	235.4	292.5
341	-	-	033	-	-	125	-	-
431	-	-	133	-	136.2	215	-	-
251	-	55.7	313	-	92.9	135	-	305.0
521	-	84.8	043	723.0	708.5	315	-	278.8
161	-	241.9	233	-	-	225	-	152.4
611	-	81.9	323	-	-	045	-	522.7
351	273.9	296.2	223	-	-	235	277.0	244.9
531	-	-	143	-	202.3	325	-	-
441	-	-	413	-	43.3	-	-	-

molecules. Therefore, in the cases of the space groups  $P6_1$  and  $P6_5$ , an asymmetric unit contains three water molecules. The results are given in Table 4. The crystal structure model  $P6_1$  with gauche-gauche (gg) conformation converged to the lowest  $R$  factor 10.85%. In the cases of  $P6_122$  and  $P6_522$ , an asymmetric unit contains three water molecules, but six water molecules with weights 0.5 was also taken into consideration because the up- and down-pointing double strand helices statistically occupy a crystal site. The refinements converged to  $R$  factors given in Table 5. The lowest  $R$  values 20.96% was obtained for  $P6_122$  with gauche-gauche (gg) conformation and six water molecules, but this is far higher than the value for  $P6_1$  with gauche-gauche (gg) conformation. Consequently, it was concluded that the crystal structure model of  $P6_1$  with gauche-gauche conformation is the correct structure.

**Crystal Structure.** The crystal and molecular structures of B-amylose are shown in Figures 8 and 9,

**Table 8. Fractional Coordinates of Amylose Molecule**

atom	$x$	$y$	$z$	atom	$x$	$y$	$z$
C1	0.3909	0.8948	-0.2410	O6	0.3850	0.8715	0.1488
C2	0.4858	0.9391	-0.2420	H1	0.3707	0.9354	-0.2783
C3	0.5163	0.8849	-0.1809	H2	0.5097	0.9965	-0.1914
C4	0.4782	0.8572	-0.0509	H3	0.4986	0.8313	-0.2385
C5	0.3835	0.8160	-0.0589	H4	0.5019	0.9105	0.0092
C6	0.3470	0.7986	0.0721	H5	0.3576	0.7597	-0.1128
O1	0.2016	0.7002	0.3333	H6	0.3566	0.7520	0.1155
O2	0.5142	0.9561	-0.3683	H7	0.2816	0.7770	0.0669
O3	0.6047	0.9203	-0.1732	H8	0.4950	0.9903	-0.4069
O4	0.4987	0.7984	0.0000	H9	0.6287	0.9378	-0.2552
O5	0.3621	0.8730	-0.1163	H10	0.3604	0.8583	0.2308

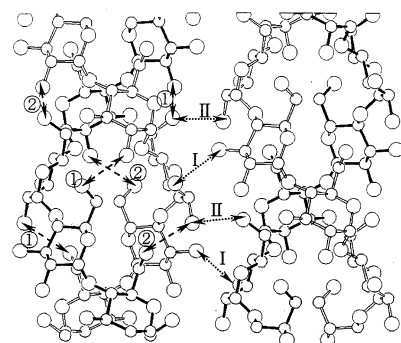
<sup>a</sup> Fractional coordinates of another residue in the same asymmetric unit are given by the following equation:

$$\mathbf{x}' = \begin{bmatrix} 0 & 1 & 0 \\ -1 & 1 & 0 \\ 0 & 0 & 1 \end{bmatrix} \mathbf{x} + \begin{bmatrix} 1/3 \\ 2/3 \\ 1/3 \end{bmatrix}$$

**Table 9. Fractional Coordinates of Water Molecules**

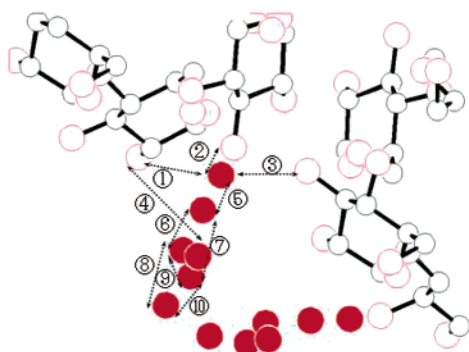
atom	$x$	$y$	$z$	atom	$x$	$y$	$z$
W1	0.0356	-0.1560	0.4707	W4	0.1539	0.0292	0.0352
W2	0.0420	-0.0576	0.1064	W5	0.2025	0.0664	0.2642
W3	0.0742	-0.2692	-0.0888	W6	0.2778	0.0711	0.0961

respectively. The parameters finally obtained by the constrained least-squares method are given in Table 6. The comparison between the observed and calculated structure factors is given in Table 7. Some nonobserved reflections give larger structure factors than the threshold of the observed structure factor, which might be attributed to the ambiguity of the positions of water molecules. The atomic parameters in fractional coordinates of amylose and water are given in Tables 8 and 9, respectively. The molecular and crystal structures obtained in the present study (Figures 8 and 9) are essentially the same as the ones reported by Imberty and Perez.<sup>8</sup> The conformation of the bonds linking two glucose residues,  $\Phi$  and  $\Psi$ , are  $+84.3^\circ$  and  $-135.2^\circ$ , respectively, which correspond well to the values  $+83.8^\circ$  and  $-144.6^\circ$  and  $+84.3^\circ$  and  $-144.1^\circ$  reported by Imberty and Perez.<sup>8</sup> Here, it should be noted that, in the work reported by Imberty and Perez,<sup>8</sup> the 2-fold rotation symmetry coinciding with the 3-fold screw axis in the space group is not strictly maintained. This shows that the intensity data reported by Wu and Sarko,<sup>5</sup> which was also used by Imberty and Perez,<sup>8</sup> was measured carefully. The double strand helix was composed of two parallel strand (6/1) single helices. Two single helices in the double strand helix are bound by two hydrogen bonds between O2 and O6 atoms (Figure 10). This is the same as Imberty and Perez.<sup>8</sup> The hydroxyl group O6 assumes a gauche-gauche (gg) conformation (Figure 7). The internal rotation angle of the primary hydroxyl group is  $-65.1^\circ$ , which corresponds well to the values  $-68.4^\circ$  and  $-52.5^\circ$  in the work reported by Imberty and Perez.<sup>8</sup> The neighboring double strand helices are bound by four hydrogen bonds of O3...O3 and O2...O6 (Figure 10). The water molecules are located on the space surrounded by six double strand helices. The short contacts of the oxygen atoms of water molecules are shown in Figure 11. Water 3 (w3) bridges two neighboring double strand helices by three hydrogen bonds with O2, O3, and O2 atoms. This is different from the work reported by Imberty and Perez.<sup>8</sup> The distances between w3 and w6 and between w2 and w5 are 1.20 and 1.73 Å, respectively, which are short in comparison with the



Atom pair	distance (Å)
interstrand hydrogen bond	
① : O2---O6'	3.198
② : O6---O2'	3.197
interdouble helices hydrogen bonds	
I : O3---O3'	2.784
II : O2---O6	2.926

**Figure 10.** Hydrogen bonds between two neighboring double helices.



Atom pair	distance (Å)
① : w3---O2	3.013
② : w3---O3	2.807
③ : w3---O2	2.324
④ : w1---O2	3.927
⑤ : w3---w6	1.203
⑥ : w5---w6	2.245
⑦ : w4---w6	2.123
⑧ : w2---w5	1.727
⑨ : w4---w5	2.573
⑩ : w2---w4	2.030

**Figure 11.** Hydrogen bonds between water molecules.

sum of the van der Waals radii of oxygen atoms. Furthermore, the distance between w1 and O2 is 3.93 Å, which is too long to form the hydrogen bond. These may suggest that the positions of water molecules are

disordered in crystal. It may be considered that in the crystal, the water molecules statistically occupy two or more definite positions with different probabilities.

**Acknowledgment.** The authors express their thanks to Prof. S. Kitamura and Prof. K. Ogawa of Osaka Prefectural University for supplying the enzymatically synthesized amylose and advice for the preparation of B-amylose, respectively.

## References and Notes

- (1) Wu, C. H.; Sarko, A. *Carbohydr. Res.* **1977**, *54*, C3.
- (2) Wu, C. H.; Sarko, A. *Carbohydr. Res.* **1978**, *61*, 7.
- (3) Blackwell, J.; Sarko, A.; Marchessault, R. H. *J. Mol. Biol.* **1969**, *42*, 379.
- (4) Zugenmaier, P.; Sarko, A. *Biopolymers* **1973**, *12*, 435.
- (5) Wu, C. H.; Sarko, A. *Carbohydr. Res.* **1978**, *61*, 7.
- (6) Imberty, A.; Chanzy, H.; Perez, S.; Buleon, A.; Tran, V. *Macromolecules* **1987**, *20*, 2634.
- (7) Imberty, A.; Chanzy, H.; Perez, S.; Buleon, A.; Tran, V. *J. Mol. Biol.* **1988**, *201*, 365.
- (8) Imberty, A.; Perez, S. *Biopolymers* **1988**, *27*, 1205.
- (9) Winter, W. T.; Sarko, A. *Biopolymers* **1974**, *13*, 1447.
- (10) Zugenmaier, P.; Sarko, A. *Biopolymers* **1976**, *15*, 2121.
- (11) Rappenecker, G.; Zugenmaier, P. *Carbohydr. Res.* **1981**, *89*, 11.
- (12) Pangborn, W.; Lings, D.; Perez, S. *Int. J. Biol. Macromol.* **1985**, *7*, 363.
- (13) GeBler, K.; Takaha, T.; Klauss, K.; Smith, S. M.; Okada, S.; Sheldrick, G. M.; Saenger, W. *Proc. Natl. Acad. Sci. U.S.A.* **1999**, *96*, 4246.
- (14) Nimz, O.; GeBler, K.; Uson, I.; Saenger, W. *Carbohydr. Res.* **2001**, *336*, 141.
- (15) Takahashi, Y.; Nishikawa, S. *Macromolecules* **2003**, *36*, 8656.
- (16) Kitamura, S.; Yunokawa, H.; Mitsuie, S.; Kuge, T. *Polym. J.* **1982**, *14*, 93.
- (17) Kitamura, S. *Polymeric Materials Encyclopedia*; Salomone, J. C., Ed.; CRC Press: New York, 1996; Vol. 10, p 7915.
- (18) Blackwell, J.; Sarko, A.; Marchessault, R. H. *J. Mol. Biol.* **1969**, *42*, 379.
- (19) Senti, F. R.; Witnauer, L. P. *J. Am. Chem. Soc.* **1946**, *68*, 2407.
- (20) Senti, F. R.; Witnauer, L. P. *J. Am. Chem. Soc.* **1948**, *70*, 1438.
- (21) Sarko, A.; Marchessault, R. H. *J. Am. Chem. Soc.* **1967**, *89*, 6454.
- (22) Norman, N. *Acta Crystallogr.* **1954**, *7*, 462.
- (23) Takahashi, Y.; Sul, H. To be published.
- (24) Takahashi, Y.; Kojima, R. *Macromolecules* **2003**, *36*, 5139.
- (25) Takahashi, Y. *Macromolecules* **2003**, *36*, 8652.
- (26) Takahashi, Y.; Matsubara, Y.; Tadokoro, H. *Macromolecules* **1983**, *16*, 1588.
- (27) Takahashi, Y.; Ozaki, Y.; Takase, M.; Krigbaum, W. R. *J. Polym. Sci., Polym. Phys. Ed.* **1993**, *31*, 1135.
- (28) Takahashi, Y.; Gehoh, M.; Yuzuriha, K. *Int. J. Biol. Macromol.* **1999**, *24*, 127.
- (29) Takahashi, Y.; Ishida, T.; Furusaka, M. *J. Polym. Sci., Polym. Phys. Ed.* **1988**, *26*, 2267.
- (30) Takahashi, Y.; Sato, T.; Tadokoro, H.; Tanaka, Y. *J. Polym. Sci., Polym. Phys. Ed.* **1973**, *11*, 223.
- (31) Arnott, S.; Scott, W. E. *J. Chem. Soc., Perkin Trans. II* **1972**, 324.
- (32) Takahashi, Y. Unpublished work.

MA0490956